Prediction of Teff Yield Using a Machine Learning Approach

Adugna Necho Mulatu(✉) and Eneyachew Tamir

Computer Engineering Program, Faculty of Electrical and Computer Engineering, Bahir Dar Institute of Technology, Bahir Dar University, Bahir Dar, Ethiopia
adugna.necho@bdu.edu.et, eneyachewt@gmail.com

Abstract. Teff is one of the main ingredients in everyday food for most Ethiopians, and its production mainly depends on natural conditions of the climate, unpredictable changes in the climate, and other growth factors. Teff production is extremely variable on different occasions and creates complex scenarios for prediction of yield. Traditional methods of prediction are incomplete and require field data collection, which is costly, with the result being poor prediction accuracy. Remotely sensed satellite image data has proven to be a reliable and real-time source of data for crop yield prediction; however, these data are enormous in size and difficult to interpret. Recently, machine-learning methods have been in use for processing satellite data, providing more accurate crop prediction results. However, these approaches are used in croplands covering vast areas or regions, requiring huge amounts of cropland mask data, which is not available in most developing countries, and may not provide accurate household level yield prediction. In this article, we proposed a machine learning based Teff Yield Prediction System for smaller cropland areas using publicly available multispectral satellite images, that represent spectral reflectance information related to the crop growth status collected from different satellites (Landsat-8, Sentinel-2). For this, we have prepared our own satellite image dataset for training. A Convolutional Neural Network was developed and trained to be fit for a regression task. A training loss of 3.3783 and a validation loss of 1.6212 were obtained; in other words, the model prediction accuracy was 98.38%. This shows that our model's performance is very promising.

Keywords: Teff yield · Multispectral satellite images · Machine learning · Convolutional neural network

1 Introduction

Crop farming in Ethiopia comprises large variations in both the variety of crops and growing areas. According to a study (Alemayehu 2012), small sized crop lands constitute 96% of farm land and yield a significant portion of total production for the major crops, including teff, maize, wheat, barley, and sorghum. Among these crops, teff is the most staple food in the country, and the same study shows that teff accounts for nearly 20%

B. H. Woldegiorgis et al. (Eds.): ICAST 2022, LNICST 455, pp. 159–176, 2023.
https://doi.org/10.1007/978-3-031-28725-1_10

of the harvested land. As one of the most important elements in everyday food for most Ethiopians (Lee 2018; Nandeshwar et al. 2020), the country is considered the largest teff producer in the world (Firdisa 2016; Tamirat and Tilahun 2020). In most places, it is sown by hand with the seeds left exposed (Sate and Tafese 2016). Teff covers the largest farmland (28% of crop area) in the country (FAO 2015; Firdisa 2016; Nascimento et al. 2018; Wato 2019), but its yearly production is very low as compared to other crops (Lakew and Berhanu 2019; Tesfahun 2018).

In terms of teff production area, the largest producing regions are Amhara (around 85%) and Oromia (around 87%) (Lee 2018). These regions also constitute the largest populations that consume this crop. Teff is a warm-season annual cereal that provides significant and unique nutritional qualities for health-conscious consumers. Nonetheless, it is not yet fully exploited and its contribution to food security requires further study. Teff is a low-risk crop that can withstand a variety of biotic and abiotic challenges. It can also continue to be a reliable source of food to meet the world's rapidly rising needs. Ethiopia is currently the world's largest producer of teff and it is only in this country that it is used as a staple crop, although other continents like the US and European countries are starting to promote its production and utilization (Lee 2018). Although there is a growing interest in the global market, in comparison to other important cereals, teff productivity is quite low (14.8 q/h) (CSA (Central Statistical Authority) 2016), having a number of factors to consider, including reduced fertility of soil, improper management of fertilizers and weeds, and irregular distribution of rainfall (Fenta 2018; Wakjira 2018; Tamirat and Tilahun 2020).

Teff is, and will continue to be, the most important and highly demanded crop due to its specific benefits and increasing international attention. As a result, increased production of this remarkable crop must be prioritized. Climate and other environmental changes have an impact on teff productivity, which is largely determined by natural climate conditions, which have a significant impact on teff yield.

Crop yield estimates before actual production is necessary in regions that depend on rain-fed agriculture with climatic uncertainties for taking various policy decisions. The results of yield estimates improve the timely availability of information for food security, allowing authorities to take necessary preparations to prevent famine, particularly during natural disaster years. Traditionally, in Ethiopia, the annual estimation of crop land area and production has been conducted by ECSA (Ethiopia Central Statistical Agency) at the national level (Fikre 2015).

In addition, estimation of crop yield in general is critical for food producers, policymakers, importers/exporters, seed producers, growers, and farmers in Ethiopia to improve national food security. However, due to several complicated aspects, the task is highly difficult and varies according to growing region and time of production. Identifying and addressing the difficulties is an overriding issue for understanding the stochastic nature of crop yield and devising ways to address them. Several crop yield prediction models have been developed to enhance the accuracy of yield estimations. However, getting accuracy is not easy due to the complexity and variability of natural settings, since many factors influence crop production and hence crop output.

Due to the limitations of traditional methods, modern methods such as artificial intelligence and machine learning (ML) have been introduced for efficient crop yield prediction. Considerable research efforts have been made in applying multivariate regression, decision trees, association rule mining, and artificial neural networks for crop prediction. Many key characteristics make ML methods to be potentially applied in yield prediction problems. These methods can be used to tackle complex and nonlinear real-world classification and regression problems. Not only does machine learning provide a powerful and flexible framework for data-driven decision making, but it also allows for the integration of expert knowledge into the system (Anna 2018).

In this research, we proposed a yield prediction model for teff crop using multispectral satellite images for training the model, downloaded from different sources in different years for the selected sample sites based on a ML technique, specifically a type of deep learning algorithm called the Convolutional Neural Network (CNN) model. The selected model is trained using a series of multiple-band satellite images cropped from the downloaded satellite images for specific plots of land for the main teff growing season, which is the duration from the sewing month to before harvest month (June 25–November 30 is considered) in the selected prominent Teff growing sites in the region. For ground truth data, average teff yield data was collected for the different plots for 10 years from 2010 to 2020. Primary data was collected on site by interviewing farmers. Data from CSA and other sources was also used to verify the correctness of the data provided by the farmers.

The main contributions of the paper include:

1. A dataset consisting of multiple bands of multispectral images showing temporal variation in biomass of Teff growth for different years, from different satellite sources
2. The use of freely available satellite images for crop prediction in developing countries (which may not afford commercial satellite data), which opens a window of further research for other applications
3. The use of modern deep learning technique for Teff yield prediction purpose
4. A basic CNN model was adjusted at the output layer (replacing sigmoid activation with ReLU) to be used for a regression problem (mostly, CNNs are effectively used for classification problems)

The rest of the paper is structured as follows. In Sect. 2, different related papers are reviewed. In Sect. 3, we discussed the problem setting and model of the proposed system. In Sect. 4, step-by-step procedures for developing and implementing the model are presented. Implementation, results, and analysis are presented in Sects. 5 and 6, respectively. Section 7 provides a conclusion and future work.

2 Related Works

In many countries, traditional crop production forecasting approaches have been used to collect data from field trips and reports. However, a number of problems and challenges are associated with these methods. The subjectiveness and insufficient ground truth data of these methods expose them to the introduction of large errors. Sampling and data

collection is too costly and time consuming, and may not represent the real picture on the ground. Due to this, other methods like crop model-based monitoring systems and remote sensing-based forecasting methods (that are based on NDVI) have been drawing the attention of many researchers. Crop monitoring and yield forecasting with remote sensing in Ethiopia was largely done at the regional/national level, covering broad areas with low-resolution imagery (Rojas 2006; Greatrex 2012).

Crop yield estimation and crop growth monitoring using geospatial and remote sensing technology are used for clustered crop areas to save money and time but require accurate data, technology, and expertise. It assists growers, government agencies, and crop insurance firms in planning and contributing to the national goal of food security with the following limitations to this type of research: (1) for several years, some of the areas have lacked local level ground truth data; (2) the approach necessitates additional regression analyses based on selected machine learning algorithms; (3) future analyses based on a variety of variables such as climate, agronomic factors, crop factors (e.g., harvest index), and others, in addition to ground truth; and (4) their hypothesis was to explore the yield estimation under different scenarios based on the capability of GIS technology in conjunction with machine learning algorithms in clustered areas, however, this will require additional testing for fragmented cropping systems (Hailu et al. 2022).

Ethiopian crop agriculture grows a variety of crops in many regions of the country. According to Alemayehu's research, Ethiopia's agricultural economy depends primarily on five primary cereals such as teff, wheat, maize, sorghum, and barley, which cover 75% of total cultivated land and 29% of agricultural GDP in 2005/06 (14% of the country's overall GDP) (Alemayehu 2010). In Ethiopia, Abiy introduced a GIS and RS based crop yield prediction model for the maize crop in the south Tigray Zone derived from time series data of SPOT VEGETATION, actual and potential evapotranspiration, and rainfall estimate satellite data for the years 2003–2012. Through correlation analyses, he used the input data to validate the grain yield from CSA and processed the data to forecast maize yield and map it. He got a rainfall estimate and an average NDVI that associate to maize output with 85% and 80% of the variation, respectively, by validating the generated spectro-agro-meteorological yield model by comparing it to the estimated zone level yields from CSA (r2 = 0.88, RMSE = 1.405 qha1, and a 21% coefficient of variation) (Abiy 2014).

Aklilu et al. in (Fikre 2015) filled the gap of Abiy in (Abiy 2014) in maize yield prediction in the south Tigray Zone by developing a model to forecast wheat yield for the year 2014 for the east Arsi zone, Ethiopia using remote sensing and GIS using time series data of SPOT VEGETATION, actual and potential evapotranspiration, rainfall estimate, and satellite data for the years 2004–2013. He employed CSA ground truth data to evaluate the indices' strength, and used correlation analysis to find relationships between crop yield, spectral indices, and agrometeorological variables for wheat crops over the long wet season (Meher). He discovered indices with a strong relationship to wheat yield which are highly correlated with the average Normalized Difference Vegetation Index (NDVIa) and rainfall, with 96% and 89% correlations, respectively.

A machine learning approach has been introduced to solve the limitations of conventional, remote sensing, and geospatial methods in crop yield. One of the approaches is

deep learning. The researchers (You et al. 2017) introduced a deep learning framework for crop yield prediction models based on histograms and a Deep Gaussian Process framework to avoid spatially correlated errors and inspire other applications in remote sensing and computational sustainability using publicly available remote sensing data to improve existing techniques using hand-crafted features and a novel dimensionality reduction technique to train a CNN or LSTM. They tested the method on county-level soybean yield prediction in the United States and found that it beat other methods.

Other researchers (Sun et al. 2019) introduced a deep CNN-LSTM model using weather data, MODIS Land Surface Temperature (LST) data, MODIS Surface Reflectance (SR) data, and historical soybean yield data to train the model for both end-of-season and in-season soybean yield prediction in the CONUS at the county level. All of the training data was combined and turned into histogram-based tensors for deep learning using the Google Earth Engine (GEE). The proposed model outperformed the pure CNN or LSTM model in both end-of-season and in-season scenarios, with an average RMSE of 329.53 from 2011 to 2015 and an R2 of 0.78 for the 5 years combined.

A deep learning framework based on CNNs and RNNs was proposed in (Khaki et al. 2020) for crop yield prediction utilizing environmental data and management strategies. Utilizing historical data, the CNN-RNN model was used to forecast corn and soybean yields over the whole Corn Belt (containing 13 states) in the United States using random forest (RF), deep fully connected neural networks (DFNN), and LASSO. It had a root-mean-square-error (RMSE) of 9% and 8% of their respective average yields, respectively, significantly surpassing all other methods examined.

The authors in (Debalke and Abebe 2022) introduced a maize yield forecast model using time series data from the Moderate Resolution Imaging Spectroradiometer NDVI, actual evapotranspiration, and potential evapotranspiration, and Climate Hazards Group Infrared Precipitation, with the indicators' correctness checked against official grain yield data from CSA in Kafa Zone, Ethiopia. The average NDVI and the Climatic Hazards Group Infrared Precipitation using station data reveal significant connections with maize productivity, with correlations of 84% and 89%, respectively. The spectro-agro meteorological yield model ($r2 = 0.89$, RMSE = 1.54 qha1, and 16.7% coefficient of variation) satisfactorily matched the CSA's predicted Zone level yields.

Another prediction system based on machine learning techniques such as decision tree, multivariate logistic regression, and k-nearest neighbor model was developed in (Cedric et al. 2022) to predict by combining climatic data, meteorological data, agricultural yields, and chemical data with hyper-parameter tuning methodology for the yield crops (rice, maize, cassava, seed cotton, yams, and bananas) at the country-level in West African countries throughout the year. The decision tree model performed well with a coefficient of determination (R2) of 95.3%, while the K-Nearest Neighbor model and logistic regression performed well with R2 = 93.15% and R2 = 89.78%, respectively. As a result, the decision tree and K-Nearest Neighbor models' prediction outputs are associated with the predicted data, demonstrating the efficacy of the model.

Ayalew et al. in (Ayalew et al. 2022) proposed a hybrid CNN-DNN model and compared with other machine learning algorithms such as the XGBoost machine learning (ML), CNN-DNN, CNN-XGBoost, CNN-RNN, and CNN-LSTM how performs against

various performance criteria. They tested their findings using a publicly available soybean dataset with 395 characteristics, including meteorological and soil conditions, and 25,345 samples. The suggested model outperforms other models, with an RMSE of 0.266, MSE of 0.071, and MAE of 0.199. The model's predictions fit with an R2 of 0.87. The XGBoost model came in second place, taking less time to run than the other DL-based models.

In contrast to other approaches that use cropland masks that span broad areas, we generated and used an individual plot of land multispectral satellite image based dataset in our research. This enables farmers to anticipate teff yields based on individual households, which aids in agricultural field management. For prediction, our approach employs satellite biomass photos, which can be simply downloaded without the need for any additional software or physical field visits. CNN is most commonly employed for image classification, but it was also used for regression in our system, similar to the approach followed in (Adrian 2021), by modifying the fully connected output layer, activation function, and loss functions used in classification problems.

3 Problem Setting

The traditional technique of crop yield prediction in Ethiopia is practiced by collecting data based on field visits and reports which are subjective, costly, time consuming and prone to errors due to incomplete ground observation that leads to poor crop yield assessment and delay in reporting appropriate actions to be taken. This article proposed Teff Yield Prediction Model using Multispectral Satellite Imaging and Machine learning (ML) Approach with the following specific objectives: 1) Preparation of dataset that consists of multitude of multi-layer data from different sources 2) Devising data fusion framework for combining input data from different sources for model training 3) Exploring appropriate ways of combining ML and statistical methods for improved accuracy 4) Design of the proposed model and 5) Implementation and testing of the model.

For training the model, we downloaded multiple bands of multispectral images of the selected areas from different sources, in different years for the selected sites. The multispectral bands used are related to temporal variation in biomass. The machine learning model is trained using a series of multiple-band satellite images cropped from the downloaded satellite images for specific plots of land for the main Teff growing season, which is the duration from the sewing month to before harvest month (June 25–November 30 is considered) in the selected prominent Teff growing sites in the region. For ground truth data, average teff yield data was collected for the different plots for 10 years from 2010 to 2020, with primary data collected on site, by interviewing farmers. Data from CSA and other sources was also used to verify the correctness of the data provided by the farmers.

One of the biggest challenges in data collection was obtaining an exact source of data for the specific plot, since not enough documented information was available from the farmers, agricultural extension workers, or even from woreda agricultural offices. Therefore, we had to rely on the interviews with farmers and agricultural extension workers for ground truth data preparation. Another challenge was that a specific plot of land does not grow Teff continuously (as farmers use crop rotation, or leaving the

land fallow to reduce soil stress). This creates a set of satellite image data outliers since different crops were grown and harvested during the rotation season, and since the biomass images of Teff and other crops/non-crops.

For each of the five selected regions, shown in Fig. 1, we have collected both satellite image and ground truth data for ten plots in each region. The minimum plot size considered was 1ha since we used free satellite data, which has poor resolution. Since the land management in the region is very fragmented, finding a plot with an area of 1ha or more was challenging. Therefore, we had to combine contiguous lands to get a larger area as used in (Mengesha et al. 2018). Totally, image data was collected for 500 satellite data from two satellites (Landsat L1, L2 and Sentinel A, B) with ground truth collected (five regions $\times$ 10 plots per region $\times$ 10 years for each plot). In each of the 500 satellite data sets, multispectral images the area of the selected plots depends on the size of the available contiguous land at each site.

Satellite data: One of the sources from which data is obtained is the Landsat Program. NASA and the US Geological Survey jointly operate the Landsat Program, which consists of a series of Earth-observing satellite missions. It is the world's largest collection of moderate-resolution remote sensing data that is continuously acquired. Landsat 8 and Landsat 9 are the currently orbiting, active satellites. The data has been obtained uninterruptedly starting from 1972 capturing different parts of the earth, and being a valuable source of information for research in various fields (U.S. Geological Survey 2020).

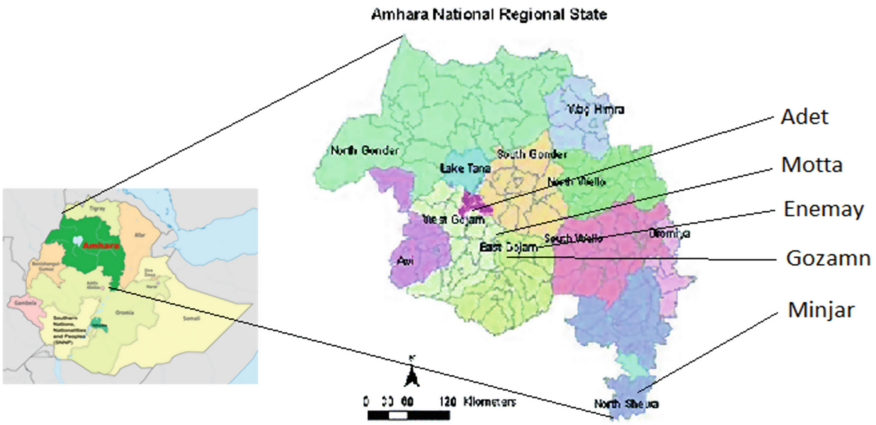

Fig. 1. Map of the study area.

For this article, we have used the Level-2 and Level-1 data from Landsat Collection 2 multispectral data. In addition, we have also used similar data downloaded from the Copernicus Sentinel-2 mission, which comprises a constellation of two polar-orbiting satellites that aim at monitoring variability in land surface conditions. This mission has a wide swath (290 km) and a high revisit time of 10 days at the equator with 1 satellite and 5 days with 2 satellites. We have downloaded data from both satellites (SA and SB) with a revisit time of nearly 5 days at the selected sites.

4 Materials and Methods

4.1 Data Sources

As previously stated, the dataset was created using multispectral temporal satellite images. As indicated in Table 1, the downloaded data includes a variety of remote sensing data, including multispectral images obtained at various bands. The whole zipped folder was downloaded for all times of visit within the given years (2005–2020). Each of the Landsat satellite's sensors was intended to collect data for a number of different frequencies in the electromagnetic spectrum. Landsat 8 measures a number of frequency bands across the electromagnetic spectrum (each range is called a band). There are numerous bands on Landsat 8. The full list of bands can be found in Table 1.

The images from the Landsat 8 Operational Land Imager (OLI) and Thermal Infrared Sensor (TIRS) have nine spectral bands, each with a spatial resolution of 30 m. Coastal and aerosol research benefit from the new band 1 (ultra-blue). The new band 9 is beneficial for detecting cirrus clouds. Band 8 (panchromatic) has a resolution of 15 m. Thermal bands 10 and 11 are collected at 100 m and are effective for delivering more accurate surface temperatures. The picture spans 170 km north to south and 183 km east to west (106 mi by 114 mi). Bands 1–9 are used to collect image data. Sentinel-2A Multispectral Instrument (MSI) data has spectral bands that are quite similar to Landsat 8 and 9 (with the exception of the thermal bands of Thermal Sentinel). The spectral bands in the Sentinel-2A Multispectral Instrument (MSI) data are fairly comparable to those in Landsat 8 and 9 (except for the thermal bands of the Thermal Infrared Sensor (TIRS)). Sample footprints acquired from Landsat and Sentinel sources are shown in Fig. 1.

Table 1. Landsat 8 list of bands

Bands	Wavelength (μm)	Resolution
B1-Coastal aerosol	0.433–0.453	30 30 m
B2-Blue	0.450–0.515	30 m
B3-Green	0.525–0.600	30 m
B4-Red	0.630–0.680	30 m
B5-Near Infrared (NIR)	0.845–0.885	30 m
B6-SWIR 1	1.560–1.660	30 m
B7-SWIR 2	2.100–2.300	30 m
B9-Cirrus	1.360–1.390	30 m
B10-Thermal Infrared (TIRS) 1	10.6–11.2	100 m
B11-Thermal Infrared (TIRS) 2	11.5–12.5	100 m

4.2 Data Collection

The coordinates used for downloading satellite data were acquired using a hand-held Garmin 70 GPS. In order to get a good resolution image and to compensate for the

moderate resolution of the publicly available satellite images, we had to search for larger contiguous plots of land. The minimum contiguous/single plot assumed was 1 Ha (100 m × 100 m). However, this gave us very poor resolution of downloaded and cropped images (e.g. only 5 × 5 pixels with a 20-m resolution satellite). The satellite data was downloaded from the U.S. Geological Survey (USGS) Earth Explorer (EE). This online earth explorer portal has a number of features including searching and browsing data online, viewing images, downloading zipped data and exporting metadata. Through enhanced user interface. Downloading was done manually by entering the coordinates and other attribute values in the USGS portal. An example attribute setting is shown in the table below, for the Motta site, plot 1. A total of more than 500 GB of 10-year data was downloaded for the 5 sites, each with 10 plots, for the different months in the harvest season of each year. Ground truth yield data was collected on site by interviewing landowners and agricultural extension workers (Table 2).

Table 2. USGS portal attribute settings/ filter criteria for downloading the plot with four corner coordinates (11.0709, 37.8955, 11.0694, 37.8972) which represent East Gojjam – Motta – Plot1

Attribute	Setting
Search Criteria	
Cloud cover	0–40%
Geocoding method	Address/Space
Shape	Predefined area
Coordinates (opposite corners – Lat, Long)	11.0709, 37.8955 11.0694, 37.8972
Dataset	
Satellites	Landsat Collection-2 Level-2, Landsat 8-9 OLI/TIRS C2 L2
	Landsat Collection 2 Level-1, Landsat 8-9 OLI/TIRS C2 L1
	Sentinel-2

4.3 Dataset Preparation

Most research works on crop yield prediction focus on a wide area of cropland, or for a certain region, using cropland masks already available, and some are based on multispectral images taken in real time using unmanned aerial vehicles. However, both of these methods do not apply to teff since no prior data is available. On the other hand, predictions made for large areas give only a general picture of production information over a region and may not accurately indicate individual farmer yield information. Hence, we had to prepare our own dataset that represents specific plots of land, particularly for the teff crop. For this purpose, we used the data from multispectral bands of satellite

images downloaded from the two satellites. The satellites used for remote sensing crop growth images have sophisticated sensing instruments that allow them to capture detailed information about the biomass on the earth's surface.

The Landsat-8 satellite uses Operational Land Imager (OLI) and the Thermal Infrared Sensor (TIRS) sensors for acquisition of seasonal coverage of the global landmass at a spatial resolution of 30 m (visible, NIR, SWIR) [landsat.gsfc.nasa.gov/satellites/landsat-8/]; 100 m (thermal); and 15 m (panchromatic) of different bands at different wavelengths of the electromagnetic spectrum. The downloaded data contains a large amount of information, but we only used the 9 bands: 0–9 of multispectral images. As mentioned above, the downloaded footprint covers a very large area (relative to a single plot), and the plots of land to be studied had to be cropped out of this footprint for each band, and separately stored. For cropping and analysis of the downloaded geospatial images, the open-source QGIS 3.24.2 desktop application was used. Every image was cropped manually, and a total of more than 45,000 images were cropped from the 5 sites. These images were saved in a hierarchical directory structure for clarity and ease of access. Figure 2 shows the results of sample cropped images. (The procedures for downloading and cropping and saving image data are described in Appendix-A).

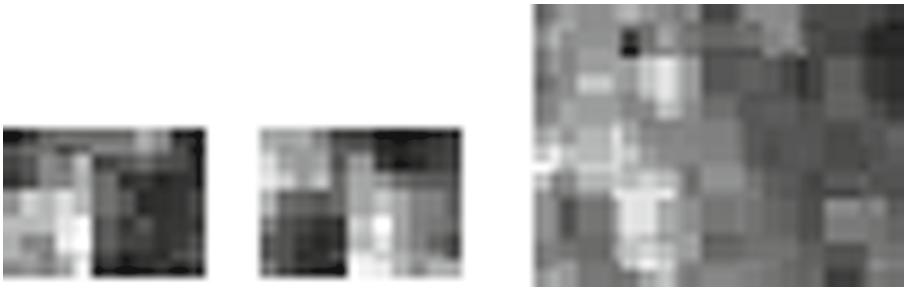

Fig. 2. Cropped images from Landsat L2 for the Gozamn area, site 1, captured on 2016-11-14, representing bands B1, B5 and B9

4.4 ML Models for Prediction

As discussed in the literature, machine learning models have proved to be much more efficient than traditional statistical models in prediction tasks. The models provide various supervised and unsupervised techniques to predict future outcomes from historical data by employing predictive models of regression. In regression, relationships between two or more variables (dependent/target and independent/predictor) are estimated, by discovering key patterns in data sets, and using simple linear regressions or complex and deep neural networks in a supervised manner.

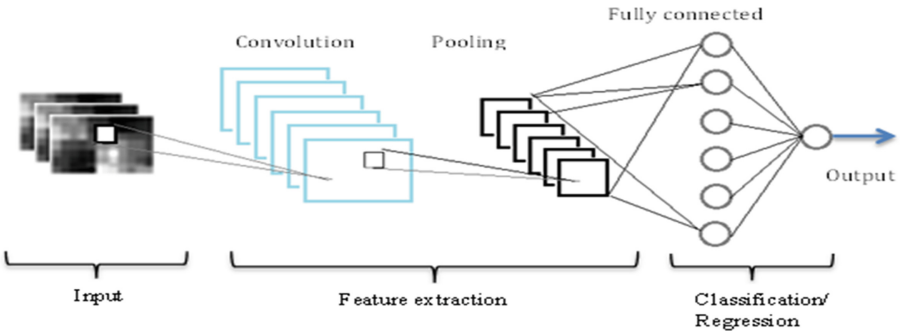

Fig. 3. The basic architecture of the CNN based teff yield prediction model

Deep learning, a branch of machine learning, is currently the most widely used model in various applications due to its various features, including its adjustable model parameters, powerful features learning ability, and end-to-end learning capability. Deep learning relies on model training based on an objective function that is related to the purpose of the model. A number of different types of deep learning models have been in use, but the Convolutional Neural Networks (CNNs) are becoming more and more efficiently employed in crop prediction tasks. CNNs can handle large amounts of complex labeled input, including image data, and computation.

The basic architecture of CNN consists of input, feature extraction, and classification/regression components (Fig. 3). Input data is represented as a multidimensional array and every portion of an input image is extracted by assigning input neurons, which are called receptive fields. The feature extraction layer consists of convolution, which produces feature maps, and a pooling layer, which reduces features. The classification layer consists of a fully connected network and an output layer. The convolution layer creates feature maps out of input data. Feature maps are filtered by applying a convolution operation using a convolution filter, which is a weight matrix that extracts certain features from the input image. The pooling layer decreases the size of the feature map by reducing the spatial size of images, which reduces computational cost. The Fully Connected (FC) layer consists of the weights and biases along with the neurons and is used to connect the neurons between two different layers.

The different steps of training algorithm:

1. Prepare dataset:
   Preprocess images (cloud cover removal, image resizing to 32x32 pixels).
2. Import necessary modules from Keras and other libraries
3. Load dataset:
   Divide dataset into training and testing sets;
   Load variables: train_input, train_target, test_input, test_target;
4. Process data:
   Normalize pixel intensity to [0,1]
   Reshape array into appropriate dimensions (instances, pixels(x,y), channels)
5. Create sequential model:
   Model = sequential()
   Init number of layers;
   For each layer,
      Create layers: CONVOLUTION, ReLU, Batch_N, MAX_ POOL
      X=Convolve_2D(train_input)
      X=Activation(ReLU)(train_input)
      X=Batch_Normalization(train_input)
      X=Max_Pooling2D(pool_size)
   Create dense layer for regression with linear activation
   Create single output layer
   Construct model: Model(inputs, x)
6. Compile model:
   Loss function = Mean_Sq_Err, Mean_Abs_Err
   Model_Optimizer = Adams
   Metrics = accuracy
7. Train model
   Model.fit(train_input, test_input, batch_size, num_ epochs)
8. Produce statistics:
   MSE,avg_prediction_result

5 Implementation

For implementing the prediction system, we have created a deep learning model with input, hidden, and output layers. The model was created using Keras and Tensorflow tools. The algorithm was implemented using Python and the Jupyter Notebook environment. Due to resource limitations on our local machines, a Google Colab notebook was used.

Most of the CNN models that exist in literature using images as input are for classification purposes. However, with some adjustments to the basic CNN architecture, CNNs can be used for regression problems similar to yield prediction. In our experiment, we used RMSE as the loss function, and replaced the sigmoid activation with ReLU to enable regression on a CNN. In addition, the output FC layer used for classification has to be changed to a single node, since only a single value of prediction is expected. The sigmoid function for the output layer is also replaced with linear regression. For optimization, we used the Adam optimizer with a learning rate of 0.001, which is fast and efficient, and has a higher convergence rate compared to other adaptive models.

Model definition: The implemented CNN model consists of the following layers: The input layer: consists of a sequence of preprocessed multispectral spatio-temporal images that represent the teff plant growth at different growth status. Since the cropped images are of variable size, the images are resized to 32×32 pixels. So the input consists of 32×32 pixels, single channel image data. The convolution layer: extracts valuable features from the input image. Multiple layers of convolutions were tested, using 3×3 filters. Pooling layer: Max pooling operation with 2×2 windows was used. Model hyper

parameters**:** In CNN (and other ML models), there are a number of hyper parameters that are required to configure the model. The research in (Aszemi and Dominic 2019) summarizes two classes of hyper parameters listed below:

a) Hyper parameters that determine the network architecture:

- *Kernel Size* – convolution filter size.
- *Stride* – number of steps the kernel moves over the input image.
- *Padding* – adding 0s at the borders of the image to account for filtering the edge of the image.
- *Hidden layers—layers* the sequence of convolution layers between input and output layers.
- *Activation functions* – allow the model to learn nonlinear prediction boundaries.

b) Hyper parameters that determine the network training:

- *Learning rate* – determines how weights are updated.
- *Momentum* – determines how the previous weight update influences the current weight update.
- *Number of epochs* – number of iterations of the entire training.
- *Batch size* – the number of inputs to be input before the updating weight.

These parameters, which are external to the model, greatly influence model performance. However, it is very difficult to have optimal values for a specific model. So the parameters are usually set by rules of thumb or heuristics, or based on previous research recommendations. The hyper parameters used and their settings are listed in Table 3.

Table 3. Hyper parameter settings for training the CNN model

Hyper parameter	Value
Kernel size	5×5
Stride	2
Padding	Yes, 0
Number of hidden layers (COV- > ReLU- > POOLING)	12
Activation functions	ReLU for conv. Layers, linear for output
Learning rate	0.01
Batch size	30
Number of epochs	30, 100, 200, 300

6 Results and Analysis

The proposed model training was done by varying the number of epochs while keeping other parameters fixed. Table 4 shows training loss and validation loss for the different epochs used for training. The results show that clearly, for lower epochs, larger values of loss were obtained. The very promising thing is that both training and validation losses were rapidly reduced as the epoch increased. This is also shown in Fig. 4a–d. However, at 300 epochs, unstable validation loss is observed as shown in Fig. 4d, so the best result obtained was at 200 epochs, with a training loss of 3.3783 and a validation loss of 1.6212.

Table 4. MSE for the different epochs tested during training

No. of epochs	30	100	200	300
Training loss (%)	55.15	13.42	3.38	1.24
Validation loss (%)	8.05	2.37	1.62	1.23

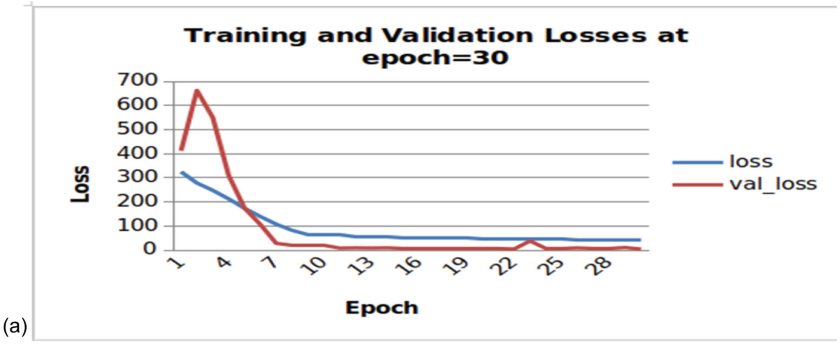

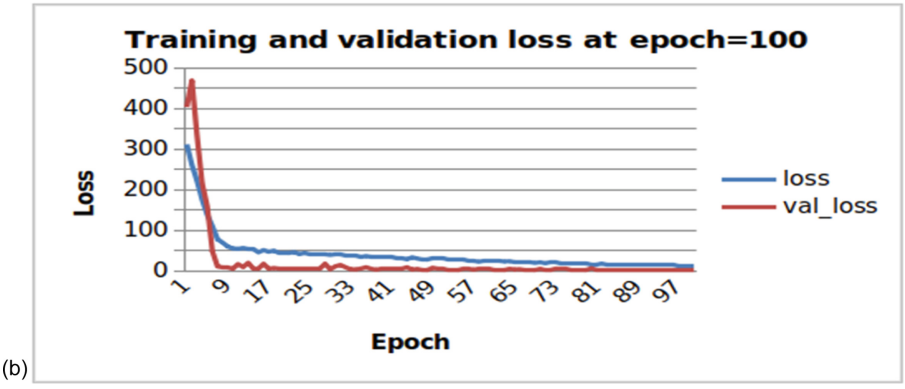

Fig. 4. Training and validation losses at different epochs of: (a) 30, (b) 100, (c) 200, (d) 300

(c)

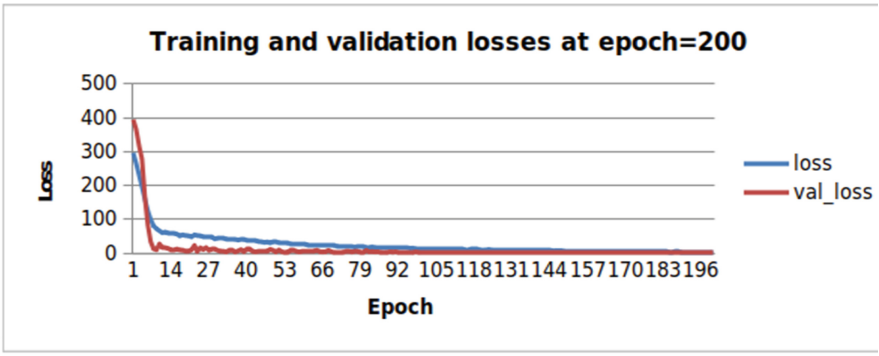

(d)

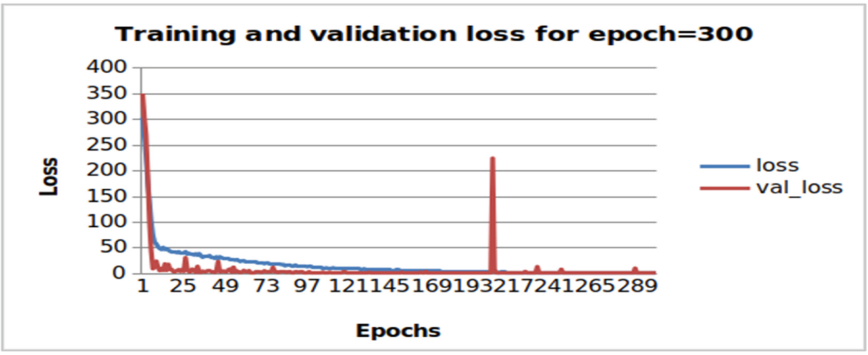

Fig. 4. (*continued*)

7 Conclusion and Future Work

In this research, we have implemented a machine learning based teff yield prediction system using multispectral satellite images collected from different satellites (Landsat-8, Sentinel-2). For this, we have prepared our own satellite image dataset for training. A CNN network was trained, with some modifications of the model to fit for regression. A training loss of 3.3783 and a validation loss of 1.6212 were obtained; in other words, the model prediction accuracy was 98.38. This shows that our model's performance is very promising. The results can be further improved and used for implementing household level yield prediction systems, such as mobile apps, so that farmers can use it for cropland management.

This work is only a start in teff yield prediction using a machine learning approach and can be extended or improved in a number of ways. A machine learning model is as accurate as the quality of training data. We have used only representative data and fewer samples from sample sites. The accuracy was obtained using satellite image data only. This accuracy can be further improved in a number of aspects. First, a large amount of dataset is required for training the CNN, so preparing such a dataset that incorporates many teff-growing regions in the country is a huge task that requires expertise and

budget. On the other hand, one can extend this work for better results by incorporating environmental and soil data with the image data for training, using data fusion techniques.

Implementing and testing machine learning-based regression algorithms other than CNN could also be another future work. The trained model can also be used as a good starting point for prediction of teff yield in other regions of the country, by applying techniques like transfer learning. Apart from that, the dataset can be enriched by using more accurate remote sensing images of specific croplands taken using unmanned aerial vehicles. Due to time and budget constraints, we were not able to develop a mobile app for household level prediction purposes. In the future, we plan to develop such an app that integrates with the system, and provides yield prediction at any stage of the growth of teff to the farmers, by acquiring the most recent available satellite image data.

Acknowledgments. This research was fully funded by Bahir Dar Institute of Technology, BiT, Bahir Dar University, and we would like to acknowledge BiT for providing the funding.

Appendix-A: Training Progress for 30 Epochs

```
Epoch 1/30
120/120 [==============================] -5s 16ms/step-loss: 305.3471-val_loss: 382.2482
Epoch 2/30
120/120 [==============================] -2s 14ms/step-loss: 256.0030-val_loss: 381.8294
Epoch 3/30
120/120 [==============================] -2s 13ms/step-loss: 216.2533-val_loss: 327.8867
Epoch 4/30
120/120 [==============================] -2s 13ms/step-loss: 174.1100-val_loss: 233.1403
Epoch 5/30
120/120 [==============================] -2s 14ms/step-loss: 136.8061-val_loss: 134.1799
Epoch 6/30
120/120 [==============================] -2s 14ms/step-loss: 107.5622-val_loss: 55.5419
Epoch 7/30
120/120 [==============================] -2s 13ms/step-loss: 87.1361-val_loss: 22.9324
Epoch 8/30
120/120 [==============================] -2s 14ms/step-loss: 74.8587-val_loss: 12.3104
Epoch 9/30
120/120 [==============================] -2s 14ms/step-loss: 62.5622-val_loss: 10.0009
Epoch 10/30
120/120 [==============================] -2s 14ms/step-loss: 64.1516-al_loss: 10.5025
Epoch 11/30
120/120 [==============================] -2s 13ms/step-loss: 60.1122-val_loss: 6.8759
Epoch 12/30
120/120 [==============================] -2s 13ms/step-loss: 59.9180-val_loss: 9.5608
Epoch 13/30
120/120[==============================] -2s 14ms/step-loss: 55.1472-val_loss: 8.0470
```

Appendix-B: Sample Ground Truth Data from CSA

Places	Year	2013/14	2014/15	2015/16	2016/17	2017/18	2018/19	2019/20	2020/21
	Ethiopia	14.65	15.75	15.6	16.64	17.48	17.56	18.5	18.82
	Amhara	14.95	15.83	16.07	16.99	17.92	18	18.94	19.3
	North Shewa	15.13	16.88	16.51	17.8			18.95	21.06
	p1	14	15.2	16.4	17.2			19.3	20.1
	p2	15	16.2	16.3	17.1			19.2	20.9
CSA	p10	15.5	16.1	16	17.3			18.7	21.66
Minjar	East Gojam	17.14	17.39	18.53	19.23			20.76	22.65
	p1	17.3	17.4	18.3	19.1			20.8	22.5
.	p2	17.2	16.1	18.8	18.31			20.3	22.1
	p10	17.1	17.3	17.7	20.1			21.3	22.42
	p1	18.1	18.2	18.3	20.3			22.1	23.2
Mota	p2	17.2	17.4	18.1	19.4			19.8	23.1
	p10	17.6	17.9	18.7	18.9			20.3	22.7
	p1	17.14	17.39	18.53	19.23			20.76	22.65
	p2	17.1	17.4	18.6	19.3			20.8	22.7
	p10	18.1	17.6	19.22				20.91	22.5
	West Gojam	13.58	15.77	16.1	17.22			20.57	20.4
	p1	13.8	14.6	16.2	17.1			19.88	20.5
	p2	14.1	15.5	16.51	17.3			19.45	20.4
Enebisie	p10	13.6	15.77	17.2	18.44			19.33	20

References

Taffesse, A.S., Dorosh, P., Gemessa, S.A.: Crop production in Ethiopia: regional patterns and trends. In: Food and Agriculture in Ethiopia: Progress and Policy Challenges, pp. 53–83 (2012)

Chilingaryan, A., Sukkarieh, S., Whelan, B.: Machine learning approaches for crop yield prediction and nitrogen status estimation in precision agriculture: a review. Comp. Electr. Agric. **151**, 61–69 (2018)

Rojas, O.: Operational maize yield model development and validation based on Remote sensing and agrometeorological data in Kenya. In: Proceedings of Remote Sensing Support to Crop yield Forecast and Area Estimates Workshop (2006)

Greatrex, H.: The Application of Seasonal Rainfall Forecasts and Satellite Rainfall Estimates to Seasonal Crop Yield Forecasting for Africa. PhD Dissertation, University of Reading, Reading, UK (2012)

Wgderes, A.: Maize Yield Forecasting in South Tigray, M.Sc. Thesis Addis Ababa University. Addis Ababa, Ethiopia (2014)

Fikre, A.: Wheat Yield Forecast Using Remote Sensing and GIS In East Arsi Zone, Ethiopia (2015)

Lee, H.J.: Teff, a rising global crop: current status of teff production and value chain. Open Agric. J. **12**(1), 185–193 (2018). https://doi.org/10.2174/1874331501812010185

Debalke, D.B., Abebe, J.T.: Maize yield forecast using GIS and remote sensing in Kaffa Zone, South West Ethiopia. Environ. Syst. Res. **11**(1), 1–16 (2022). https://doi.org/10.1186/s40068-022-00249-5

Cedric, L.S., et al.: Crops yield prediction based on machine learning models: case of West African countries. Smart Agric. Technol. 100049 (2022)

Sun, J., Di, L., Sun, Z., Shen, Y., Lai, Z.: County-level soybean yield prediction using deep CNN-LSTM model. Sensors **19**(20), 4363 (2019). https://doi.org/10.3390/s19204363

You, J., Li, X., Low, M., Lobell, D., Ermon, S.: Deep gaussian process for crop yield prediction based on remote sensing data. In: Thirty-First AAAI conference on Artificial Intelligence (2017)

Hailu, S., Getachew, T., Habtamu, S., Leulseged, T.: Crop yield estimation of teff (Eragrostis tef Zuccagni) using geospatial technology and machine learning algorithm in the central highlands of Ethiopia. Sustain. Agric. Res. **11**(1), 1–34 (2022)

Sewnet, H., Tesfaye, G., Shiferaw, H., Tamene, L.: Phenology based Time Series LAI as a Proxy for Teff Crop Yield Estimation: A Case in Major Teff (Eragrostis) Growing Zones of Ethiopia, p. 30 (2021)

Tesfaye, G., Sewnet, H., Shiferaw, H, Desta, L., Abera, W., Gudeta, K.: Tef yield estimation based on satellite-derived light use efficiency model. A case study in the top tef growing zones of Ethiopia, p. 38 (2021)

Pantazi, X.E., Moshou, D., Alexandridis, T., Whetton, R.L., Mouazen, A.M.: Wheat yield prediction using machine learning and advanced sensing techniques. Comput. Electron. Agric. **121**, 57–65 (2016). https://doi.org/10.1016/j.compag.2015.11.018

Battude, M.: Estimating maize biomass and yield over large areas using high spatial and temporal resolution Sentinel-2 like remote sensing data. Remote Sens. Environ. **184**, 668–681 (2016). https://doi.org/10.1016/j.rse.2016.07.030

Fenta, A.: Effect of Teff variety and rates of nitrogen fertilizer application on growth and yield components under Jimma condition. ARPN J. Agri. Biol. Sci. **13**(3), 42–43 (2018)

Nandeshwar, B.C., et al.: Teff (Eragrostis tef [Zucc] Trotter): an emerging global demanding crop. Agric. Observer **1**(1), 28–33 (2020)

Tadesse, D., Alem, T., Wossen, T.: Evaluation of improved varieties of Teff in West Belesa, Northwest Ethiopia. Rev. Plant Stud. **3**, 1–6 (2016). https://doi.org/10.18488/journal.69/2016.3.1/69.1.1.6

Tamirat, W., Tilahun, N.: The response of Teff [Eragrostis teff (Zucc.) trotter] to nitrogen fertilizer and development of Barley (Hordeum vulgare L.) at Bore district, Southern Oromia, Ethiopia. American J. Life Sci. **2**(5), 260–266 (2020). https://doi.org/10.11648/j.ajls.20140205.12

Tesfahun, W.: Tef yield response to NPS fertilizer and methods of sowing in East Shewa, Ethiopia. J. Agri. Sci. Sri Lanka **13**(2), 162–173 (2018). https://doi.org/10.4038/jas.v13i2.8340

Wato, T.: Effects of nitrogen fertilizer rate and inter-row spacing on yield and yield components of teff [Eragrostis teff (Zucc.) Trotter] in Limo district, Southern Ethiopia. Int. J. Plant Soil Sci. **31**(3), 1–12 (2019). https://doi.org/10.9734/IJPSS/2019/v31i330211

Khaki, S., Wang, L., Archontoulis, S.V.: A CNN-RNN framework for crop yield prediction. Front. Plant Sci. **10**, 1750 (2020). https://doi.org/10.3389/fpls.2019.01750

Wato, T., Moral, M.T. (Reviewing ed.): Tef [Eragrostis tef (Zucc)] grain yield response to nitrogen fertilizer rates in East Badewacho district, Hadiya Zone, Southern Ethiopia. Cogent Food Agric. **7**, 1 (2021). https://doi.org/10.1080/23311932.2021.1909203

Cochrane, L., Bekele, Y.W.: Average crop yield (2001–2017) in Ethiopia: trends at national, regional and zonal levels. Data Brief **16**, 1025 (2018)

Alexandros, O., Cagatay, C., Ayalew, K.: Hybrid deep learning-based models for crop yield prediction. Appl. Artif. Intell. (2022). https://doi.org/10.1080/08839514.2022.2031823

Meshesha, D.T., Abeje, M.: Developing crop yield forecasting models for four major Ethiopian agricultural commodities. Remote Sens. Appl. Soc. Environ. support52938517302434. https://doi.org/10.1016/j.rsase.2018.05.001 (2018)

Rosebrock, A.: https://pyimagesearch.com/2019/01/28/keras-regression-and-cnns/. Accessed 7 May 2022(2021)

U.S. Geological Survey: https://pubs.er.usgs.gov/publication/fs20153081. Accessed 7 May 2022. Revised (April 8, 2020)

Aszemi, N.M., Dominic, P.D.D.: Hyperparameter optimization in convolutional neural networks using genetic algorithms. Int. J. Adv. Comput. Sci. Appl **10**(6), 269–278 (2019)

The US Geological Survey: www.usgs.org